Measurement of the b forward-backward asymmetry and mixing using high-p⊥ leptons

BUSKULIC, D.

M. THULASIDAS
Singapore Management University, manojt@smu.edu.sg

Citation
1

EUROPEAN LABORATORY FOR PARTICLE PHYSICS

Measurement of the b forward–backward asymmetry and mixing using high–$p_\perp$ leptons

The ALEPH Collaboration

Abstract

The $B^0 - \overline{B}^0$ average mixing parameter $\overline{\chi}$ and b forward–backward asymmetry $A^0_{FB}(b)$ are measured from a sample of about 4,200,000 $Z \to q\overline{q}$ events recorded with the ALEPH detector at LEP in the years 1990–1995. High transverse momentum electrons and muons produced in b semileptonic decays provide the tag of the quark flavour and of its charge.

The average mixing parameter and the pole b asymmetry are measured to be

$$\overline{\chi} = 0.1246 \pm 0.0051\,_{\text{stat}} \pm 0.0052\,_{\text{syst}},$$
$$A^0_{FB}(b) = 0.1008 \pm 0.0043\,_{\text{stat}} \pm 0.0028\,_{\text{syst}}.$$

The value of $\sin^2\theta^{\text{eff}}_W = 0.23198 \pm 0.00092$ is extracted from the asymmetry measurement.

Submitted to Phys. Lett. B

The ALEPH Collaboration

D. Buskulic, I. De Bonis, D. Decamp, P. Ghez, C. Goy, J.-P. Lees, A. Lucotte, M.-N. Minard, P. Odier, B. Pietrzyk

Laboratoire de Physique des Particules (LAPP), IN^{2}P^3-CNRS, 74019 Annecy-le-Vieux Cedex, France

M.P. Casado, M. Chmeissani, J.M. Crespo, M. Delfino,[12] I. Efthymiopoulos,[1] E. Fernandez, M. Fernandez-Bosman, Ll. Garrido,[15] A. Juste, M. Martinez, S. Orteu, A. Pacheco, C. Padilla, A. Pascual, J.A. Perlas, I. Riu, F. Sanchez, F. Teubert

Institut de Fisica d'Altes Energies, Universitat Autonoma de Barcelona, 08193 Bellaterra (Barcelona), Spain[7]

A. Colaleo, D. Creanza, M. de Palma, G. Gelao, M. Girone, G. Iaselli, G. Maggi,[3] M. Maggi, N. Marinelli, S. Nuzzo, A. Ranieri, G. Raso, F. Ruggieri, G. Selvaggi, L. Silvestris, P. Tempesta, G. Zito

Dipartimento di Fisica, INFN Sezione di Bari, 70126 Bari, Italy

X. Huang, J. Lin, Q. Ouyang, T. Wang, Y. Xie, R. Xu, S. Xue, J. Zhang, L. Zhang, W. Zhao

Institute of High-Energy Physics, Academia Sinica, Beijing, The People's Republic of China[8]

R. Alemany, A.O. Bazarko, G. Bonvicini,[23] M. Cattaneo, P. Comas, P. Coyle, H. Drevermann, R.W. Forty, M. Frank, R. Hagelberg, J. Harvey, P. Janot, B. Jost, E. Kneringer, J. Knobloch, I. Lehraus, E.B. Martin, P. Mato, A. Minten, R. Miquel, Ll.M. Mir,[2] L. Moneta, T. Oest,[20] F. Palla, J.R. Pater,[27] J.-F. Pusztaszeri, F. Ranjard, P. Rensing, L. Rolandi, D. Schlatter, M. Schmelling,[24] O. Schneider, W. Tejessy, I.R. Tomalin, A. Venturi, H. Wachsmuth, A. Wagner, T. Wildish

European Laboratory for Particle Physics (CERN), 1211 Geneva 23, Switzerland

Z. Ajaltouni, A. Barrès, C. Boyer, A. Falvard, P. Gay, C . Guicheney, P. Henrard, J. Jousset, B. Michel, S. Monteil, J-C. Montret, D. Pallin, P. Perret, F. Podlyski, J. Proriol, J.-M. Rossignol

Laboratoire de Physique Corpusculaire, Université Blaise Pascal, IN^{2}P^3-CNRS, Clermont-Ferrand, 63177 Aubière, France

T. Fearnley, J.B. Hansen, J.D. Hansen, J.R. Hansen, P.H. Hansen, B.S. Nilsson, A. Wäänänen

Niels Bohr Institute, 2100 Copenhagen, Denmark[9]

A. Kyriakis, C. Markou, E. Simopoulou, I. Siotis, A. Vayaki, K. Zachariadou

Nuclear Research Center Demokritos (NRCD), Athens, Greece

A. Blondel, G. Bonneaud, J.C. Brient, P. Bourdon, A. Rougé, M. Rumpf, A. Valassi,[6] M. Verderi, H. Videau[21]

Laboratoire de Physique Nucléaire et des Hautes Energies, Ecole Polytechnique, IN^{2}P^3-CNRS, 91128 Palaiseau Cedex, France

D.J. Candlin, M.I. Parsons

Department of Physics, University of Edinburgh, Edinburgh EH9 3JZ, United Kingdom[10]

E. Focardi,[21] G. Parrini

Dipartimento di Fisica, Università di Firenze, INFN Sezione di Firenze, 50125 Firenze, Italy

M. Corden, C. Georgiopoulos, D.E. Jaffe

Supercomputer Computations Research Institute, Florida State University, Tallahassee, FL 32306-4052, USA [13,14]

A. Antonelli, G. Bencivenni, G. Bologna,[4] F. Bossi, P. Campana, G. Capon, D. Casper, V. Chiarella, G. Felici, P. Laurelli, G. Mannocchi,[5] F. Murtas, G.P. Murtas, L. Passalacqua, M. Pepe-Altarelli

Laboratori Nazionali dell'INFN (LNF-INFN), 00044 Frascati, Italy

L. Curtis, S.J. Dorris, A.W. Halley, I.G. Knowles, J.G. Lynch, V. O'Shea, C. Raine, P. Reeves, J.M. Scarr, K. Smith, A.S. Thompson, F. Thomson, S. Thorn, R.M. Turnbull

Department of Physics and Astronomy, University of Glasgow, Glasgow G12 8QQ,United Kingdom[10]

U. Becker, C. Geweniger, G. Graefe, P. Hanke, G. Hansper, V. Hepp, E.E. Kluge, A. Putzer, B. Rensch, M. Schmidt, J. Sommer, H. Stenzel, K. Tittel, S. Werner, M. Wunsch

Institut für Hochenergiephysik, Universität Heidelberg, 69120 Heidelberg, Fed. Rep. of Germany[16]

D. Abbaneo, R. Beuselinck, D.M. Binnie, W. Cameron, P.J. Dornan, A. Moutoussi, J. Nash, J.K. Sedgbeer, A.M. Stacey, M.D. Williams

Department of Physics, Imperial College, London SW7 2BZ, United Kingdom[10]

G. Dissertori, P. Girtler, D. Kuhn, G. Rudolph

Institut für Experimentalphysik, Universität Innsbruck, 6020 Innsbruck, Austria[18]

A.P. Betteridge, C.K. Bowdery, P. Colrain, G. Crawford, A.J. Finch, F. Foster, G. Hughes, T. Sloan, M.I. Williams

Department of Physics, University of Lancaster, Lancaster LA1 4YB, United Kingdom[10]

A. Galla, A.M. Greene, K. Kleinknecht, G. Quast, B. Renk, E. Rohne, H.-G. Sander, P. van Gemmeren C. Zeitnitz

Institut für Physik, Universität Mainz, 55099 Mainz, Fed. Rep. of Germany[16]

J.J. Aubert,[21] A.M. Bencheikh, C. Benchouk, A. Bonissent,[21] G. Bujosa, D. Calvet, J. Carr, C. Diaconu, F. Etienne, N. Konstantinidis, P. Payre, D. Rousseau, M. Talby, A. Sadouki, M. Thulasidas, K. Trabelsi

Centre de Physique des Particules, Faculté des Sciences de Luminy, IN^2P^3-CNRS, 13288 Marseille, France

M. Aleppo, F. Ragusa[21]

Dipartimento di Fisica, Università di Milano e INFN Sezione di Milano, 20133 Milano, Italy

I. Abt, R. Assmann, C. Bauer, W. Blum, H. Dietl, F. Dydak,[21] G. Ganis, C. Gotzhein, K. Jakobs, H. Kroha, G. Lütjens, G. Lutz, W. Männer, H.-G. Moser, R. Richter, A. Rosado-Schlosser, S. Schael, R. Settles, H. Seywerd, R. St. Denis, W. Wiedenmann, G. Wolf

Max-Planck-Institut für Physik, Werner-Heisenberg-Institut, 80805 München, Fed. Rep. of Germany[16]

J. Boucrot, O. Callot, A. Cordier, M. Davier, L. Duflot, J.-F. Grivaz, Ph. Heusse, M. Jacquet, D.W. Kim,[19] F. Le Diberder, J. Lefrançois, A.-M. Lutz, I. Nikolic, H.J. Park,[19] I.C. Park,[19] M.-H. Schune, S. Simion, J.-J. Veillet, I. Videau

Laboratoire de l'Accélérateur Linéaire, Université de Paris-Sud, IN^2P^3-CNRS, 91405 Orsay Cedex, France

P. Azzurri, G. Bagliesi, G. Batignani, S. Bettarini, C. Bozzi, G. Calderini, M. Carpinelli, M.A. Ciocci, V. Ciulli, R. Dell'Orso, R. Fantechi, I. Ferrante, L. Foà,[1] F. Forti, A. Giassi, M.A. Giorgi, A. Gregorio, F. Ligabue, A. Lusiani, P.S. Marrocchesi, A. Messineo, G. Rizzo, G. Sanguinetti, A. Sciabà, P. Spagnolo, J. Steinberger, R. Tenchini, G. Tonelli,[26] C. Vannini, P.G. Verdini, J. Walsh

Dipartimento di Fisica dell'Università, INFN Sezione di Pisa, e Scuola Normale Superiore, 56010 Pisa, Italy

G.A. Blair, L.M. Bryant, F. Cerutti, J.T. Chambers, Y. Gao, M.G. Green, T. Medcalf, P. Perrodo, J.A. Strong, J.H. von Wimmersperg-Toeller

Department of Physics, Royal Holloway & Bedford New College, University of London, Surrey TW20 OEX, United Kingdom[10]

D.R. Botterill, R.W. Clifft, T.R. Edgecock, S. Haywood, P. Maley, P.R. Norton, J.C. Thompson, A.E. Wright

Particle Physics Dept., Rutherford Appleton Laboratory, Chilton, Didcot, Oxon OX11 OQX, United Kingdom[10]

B. Bloch-Devaux, P. Colas, S. Emery, W. Kozanecki, E. Lançon, M.C. Lemaire, E. Locci, B. Marx, P. Perez, J. Rander, J.-F. Renardy, A. Roussarie, J.-P. Schuller, J. Schwindling, A. Trabelsi, B. Vallage

CEA, DAPNIA/Service de Physique des Particules, CE-Saclay, 91191 Gif-sur-Yvette Cedex, France[17]

S.N. Black, J.H. Dann, R.P. Johnson, H.Y. Kim, A.M. Litke, M.A. McNeil, G. Taylor

Institute for Particle Physics, University of California at Santa Cruz, Santa Cruz, CA 95064, USA[22]

C.N. Booth, R. Boswell, C.A.J. Brew, S. Cartwright, F. Combley, A. Koksal, M. Letho, W.M. Newton, J. Reeve, L.F. Thompson

Department of Physics, University of Sheffield, Sheffield S3 7RH, United Kingdom[10]

A. Böhrer, S. Brandt, V. Büscher, G. Cowan, C. Grupen, G. Lutters, J. Minguet-Rodriguez, F. Rivera,[25] P. Saraiva, L. Smolik, F. Stephan,

Fachbereich Physik, Universität Siegen, 57068 Siegen, Fed. Rep. of Germany[16]

M. Apollonio, L. Bosisio, R. Della Marina, G. Giannini, B. Gobbo, G. Musolino,

Dipartimento di Fisica, Università di Trieste e INFN Sezione di Trieste, 34127 Trieste, Italy

J. Rothberg, S. Wasserbaech

Experimental Elementary Particle Physics, University of Washington, WA 98195 Seattle, U.S.A.

S.R. Armstrong, L. Bellantoni,[30] P. Elmer, Z. Feng,[31] D.P.S. Ferguson, Y.S. Gao,[32] S. González, J. Grahl, T.C. Greening, J.L. Harton,[28] O.J. Hayes, H. Hu, P.A. McNamara III, J.M. Nachtman, W. Orejudos, Y.B. Pan, Y. Saadi, M. Schmitt, I.J. Scott, V. Sharma,[29] A.M. Walsh,[33] Sau Lan Wu, X. Wu, J.M. Yamartino, M. Zheng, G. Zobernig

Department of Physics, University of Wisconsin, Madison, WI 53706, USA[11]

1 Introduction

The forward–backward asymmetry in $Z \rightarrow b\overline{b}$ decays at the Z resonance provides a precise measurement of the electroweak mixing angle $\sin^2\theta_W$. The asymmetry in $Z \rightarrow f\overline{f}$ decays arises from the interference between the vector and axial vector coupling of the Z to the fermion pair, leading to an odd term in the angular distribution:

$$\frac{d\sigma}{d\cos\theta} \propto \left(1 + \cos^2\theta + \frac{8}{3}A_{FB}\cos\theta\right).$$

In the improved Born approximation, for $\sqrt{s} = M_Z$, the fermion asymmetry takes the approximate form

$$A_{FB}^0(f) \simeq \frac{3}{4} \frac{2v_e a_e}{v_e^2 + a_e^2} \frac{2v_f a_f}{v_f^2 + a_f^2}.$$

Among the various species of fermions, the down–type quarks have the largest forward–backward asymmetry at the Z peak, and give the highest sensitivity to the value of $\sin^2\theta_W$. The A_{FB}^b measurement is appealing experimentally because high–purity samples of $Z \rightarrow b\overline{b}$ events can be selected, while $Z \rightarrow d\overline{d}$ or $Z \rightarrow s\overline{s}$ decays are much harder to isolate.

In $Z \rightarrow b\overline{b}$ events, the presence of $B^0 - \overline{B}^0$ mixing has the effect of diluting the observable asymmetry by a factor $(1 - 2\overline{\chi})$; therefore a precise measurement of the average mixing parameter $\overline{\chi}$ is desirable, in order to reduce the systematic uncertainty on A_{FB}^b. In addition this parameter, combined with the analyses of B_d^0 and B_s^0 meson oscillations, also contributes to the knowledge of the rate at which b quarks hadronize into these types of mesons.

Semileptonic decays of the b quark, producing prompt muons and electrons of high transverse momentum $p_\perp$ with respect to the parent hadron line of flight, allow high–purity samples of $Z \rightarrow b\overline{b}$ events to be isolated, distinguishing at the same time quark from antiquark jets. Events containing pairs of opposite–hemisphere high–$p_\perp$ leptons are used to extract the mixing parameter, while the asymmetry is measured from a fit to the polar angle distribution of events containing at least one high–$p_\perp$ candidate.

After a brief discussion of the apparatus and the lepton identification, the sources of systematic uncertainties common to the two measurements are discussed in some detail. The modelling of b decays turns out to be the most critical input for the mixing measurement, while both the mixing and the asymmetry are affected by the uncertainty on charm physics. The mixing and asymmetry measurements are then described, and the extraction of $\sin^2\theta_W^{eff}$ is performed.

2 Detector description and event selection

A detailed description of the ALEPH apparatus and its performance is given in Ref. [1, 2]. A brief overview will be given here, along with some basic information on lepton identification.

A high resolution vertex detector (VDET) consisting of two layers of double–sided silicon microstrip detectors surrounds the beampipe. The two layers are 6.5 cm and 11.3 cm from the beam axis and cover 85% and 69% of the solid angle, respectively. The spatial resolution for the $r\phi$ and z projections (transverse and along the beam axis, respectively) is 12 μm at normal incidence.

Outside the vertex detector is a drift chamber (ITC) made of eight coaxial wire layers with an outer radius of 26 cm, and a large time projection chamber (TPC) which measures up to 21

three–dimensional coordinates per track in the region between 40 and 171 cm in radius. The three tracking devices are immersed in an axial magnetic field of 1.5 T provided by a superconducting solenoid; the particle momentum transverse to the beam axis is measured with a resolution of $\sigma(p_{\rm T})/p_{\rm T} = 0.0006 p_{\rm T} \oplus 0.005$ with $p_{\rm T}$ in GeV/c. The TPC also provides up to 338 measurements of the specific ionization (dE/dx) of each charged track. Electrons are separated from other charged particles by more than three standard deviations up to a momentum of 8 GeV/c.

The electromagnetic calorimeter (ECAL) is a lead–proportional chamber sandwich; it is read out by means of cathode pads connected to form $0.9° \times 0.9°$ projective towers with three segments in depth; its energy resolution is $\sigma(E)/E = 0.18/\sqrt{E} + 0.009$ with E in GeV.

Outside the ECAL is the superconducting solenoid, surrounded by the hadron calorimeter (HCAL), composed of the iron of the magnet return yoke interleaved with 23 layers of streamer tubes. Its thickness of more than 7 interaction lengths allows a good separation between hadrons and muons. Two additional double layers of streamer tubes (muon chambers), placed outside the HCAL, enhance the performance of muon identification.

The sample of Z $\to$ q$\overline{\rm q}$ events is selected as described in Ref. [3], using all the data collected by ALEPH in the years 1990–1995. A total of 4,170,685 hadronic events are selected. Within this sample, electrons are identified by the characteristic longitudinal and transverse development of their associated shower in the ECAL; the dE/dx information from the TPC enhances the hadron rejection power, while non–prompt electrons coming from photon conversions in the detector material are rejected on the basis of their kinematic and geometric properties. Muons are identified by their characteristic penetration pattern in the HCAL, and the additional three–dimensional coordinates provided by the muon chambers help in resolving the remaining ambiguities. Both electron and muon candidates are required to have a momentum greater than 3 GeV/c. The lepton identification technique is detailed in Ref. [3].

The jets are clustered using the JADE algorithm; the cut on the jet invariant mass is set to $M_{\rm jet} = 6$ GeV/c^2. The lepton transverse momentum is calculated with respect to the jet direction after removing the lepton itself, in order to achieve the best discrimination of b $\to \ell$ decays from the other lepton sources [3]. The cut is chosen by minimizing the total uncertainty on the two measured parameters, obtaining $p_\perp > 1.25$ GeV/c.

3   Event simulation and related systematics

Details about the event simulation can be found in Ref. [4]. The parameters that are relevant for the analyses presented are retuned according to the most recent experimental measurements; their estimated uncertainties are used to evaluate the systematic error on the results, following the guidelines developed by the four LEP experiments as described in Ref. [5]. Details of this procedure are given in this section.

3.1   The fragmentation of heavy quarks

The charm fragmentation is simulated using the Peterson *et al.* function [6]. The parameter $\varepsilon_{\rm c}$, which controls the shape of the function, is chosen in order to reproduce the LEP average value of the mean scaled energy of weakly–decaying charmed hadrons, $\langle X_{\rm c} \rangle = 0.49$ [7, 8]. An uncertainty of $\pm\, 0.02$ is assigned to $\langle X_{\rm c} \rangle$, as is suggested in Ref. [5]. This uncertainty is significantly larger than

the experimental error on the world average and should account for any uncertainty coming from the fragmentation model itself.

The simulated scaled energy spectrum of b hadrons is modified to reproduce the spectrum measured by the latest ALEPH model–independent analysis [9]. The statistical and systematic uncertainties on the reconstructed spectrum are propagated, source by source, to the measurements presented here, yielding an estimate of the effect of the b fragmentation which has little dependence upon theoretical assumptions.

3.2 Heavy quark production and semileptonic decay

The Monte Carlo is reweighted in order to match the LEP average value for the partial width of the Z into b quarks, $R_b = 0.2195 \pm 0.0019$ [5].

The knowledge of the semileptonic branching ratios $BR(b \to \ell)$ and $BR(b \to c \to \ell)$ is important for a correct evaluation of the sample composition. The preliminary values measured by ALEPH [10][11][1],

$$
\begin{aligned}
BR(b \to \ell) &= \left(11.34 \pm 0.13_{\,\text{stat}} \, ^{+0.49}_{-0.38}\,_{\text{syst}}\right)\% \\
BR(b \to c \to \ell) &= \left(7.86 \pm 0.19_{\,\text{stat}} \pm 0.60_{\,\text{syst}}\right)\%
\end{aligned}
$$

are used as input for the measurements presented, obtained using the same lepton identification and a common treatment of the systematics; therefore, in propagating the uncertainty to the mixing and asymmetry parameters, the common sources are unfolded, in order to correctly account for correlations. The uncorrelated part of the error is ± 0.21 and ± 0.25 for $BR(b \to \ell)$ and $BR(b \to c \to \ell)$ respectively. The statistical correlation coefficient between the two measured branching ratios $C = -0.44$ is used when combining the errors. This procedure allows a substantial reduction of the systematic error on $\overline{\chi}$; the sensitivity of the b asymmetry to the branching ratio values is, however, small compared to other sources of uncertainty.

The semileptonic branching ratio of charm decays is taken to be $BR(c \to \ell) = (9.8 \pm 0.5)\%$ [5]; for R_c the Standard Model value of 0.171 is used, and varied by 10% to evaluate the systematics.

The lepton energy spectrum in the heavy–flavoured hadron rest frame is strongly correlated with the lepton transverse momentum spectrum measured in the laboratory frame. The lepton energy spectra in the $b \to \ell$ and $c \to \ell$ decays are reweighted to match the experimental measurements of CLEO [12], DELCO [13] and MARK III [14]. For the $b \to c \to \ell$ decay chain, the $c \to \ell$ spectrum is combined with the $b \to D$ spectrum measured from CLEO [15]. The procedure to correct the Monte Carlo and evaluate the systematic uncertainties coming from these sources is explained in Ref. [5].

3.3 Jets in charm events

The choice of the jet invariant–mass cut $M_{\text{jet}} = 6$ GeV/c^2, and the definition of the transverse momentum of the lepton with respect to the jet axis computed after removing the lepton itself, are both tailored in order to optimize the separation of the $b \to \ell$ decays from the other sources of leptons, as discussed in Ref. [3]. In the case of $c \to \ell$ decays, the mass of the heavy–flavoured

---

[1]Three measurements are described in this reference; the one with the closest treatment of the systematic errors to that presented here is used.

3

hadron is low compared to the jet invariant mass and therefore several fragmentation tracks are often absorbed in the jet. This, together with the low average multiplicity of charm decays, often causes the axis of the jet − lepton system to be dominated by the fragmentation tracks, whose simulation is therefore another important ingredient for a correct description of the measured c → ℓ transverse momentum spectrum.

This source of uncertainty is studied by selecting fast D* ($E_{D*}/E_{beam} > 0.5$) in the channel D* → D^{0}π, D^0 → Kπ, with the selection cuts described in Ref. [7]: this yields a charm purity of about 80%. The transverse momentum spectrum of the D*'s with respect to the remaining tracks in the jet is measured in the data and in the Monte Carlo. The comparison provides corrections which are applied as weights to simulated events, as well as an estimate of the associated uncertainty. The measured spectra in the data and in the Monte Carlo are shown in Fig. 1a, along with their ratio.

3.4 Other prompt leptons in b events

The fraction of b quarks decaying via a b → u transition is set to $(3 \pm 2)\%$, based on V_{ub} measurements from CLEO and ARGUS [16]. As far as lepton production is concerned, the Monte Carlo is reweighted in order to equalize the semileptonic branching ratios in b → u and b → c transitions.

The rate of leptons coming from the b → W$^-$ → $\overline{c}$ chain is set to $(1.3 \pm 0.5)\%$ as suggested in Ref. [5].

The latest ALEPH measurements BR(b → $\tau^- \overline{\nu}_\tau$X) = $(2.75 \pm 0.48)\%$ [17] and BR(b → J/ψ X) = $(1.21 \pm 0.15)\%$ [18] are used. The experimental errors are propagated to evaluate the corresponding systematic uncertainties.

3.5 Gluon splitting to heavy quarks

Charm and b quark pairs may be produced from radiated gluons. The JETSET prediction for the rate at which this process occurs is $N(g \to b\overline{b}) = 1.6 \times 10^{-3}$ and $N(g \to c\overline{c}) = 1.6 \times 10^{-2}$, where N is the number of splittings per hadronic event. The value of $N(g \to c\overline{c}) = (2.27 \pm 0.28 \pm 0.41) \times 10^{-2}$ measured by OPAL [19] is used; an uncertainty of 100% is assigned to the JETSET rate of g → b$\overline{b}$.

3.6 The $(p, p_\perp)$ spectrum of charged tracks

The rate and $p_\perp$ spectrum of charged tracks which fulfil the lepton selection kinematic cuts are checked in the data separately for Z → b$\overline{b}$, Z → c$\overline{c}$ and light quark events, in order to achieve a more reliable estimate of the lepton background and of its uncertainty.

For light quark events, a light flavour tag is applied on one hemisphere: the combined probability P_H that charged tracks belonging to the tag hemisphere come from the primary vertex (defined in Ref. [20]) is computed, and a cut at $\log P_H > -0.35$ is applied. In addition the total visible momentum of the hemisphere (including neutrals) is required to be $p_H^{vis} > 42$ GeV/c, in order to reject hemispheres with hard neutrinos. The $p_\perp$ spectrum of charged tracks belonging to the opposite hemisphere is then measured in data and Monte Carlo.

Similarly, Z → b$\overline{b}$ events are selected through a cut at $\log P_H < -4$ applied in one hemisphere. In this case leptons in the opposite hemisphere are removed by applying loose lepton identification

4
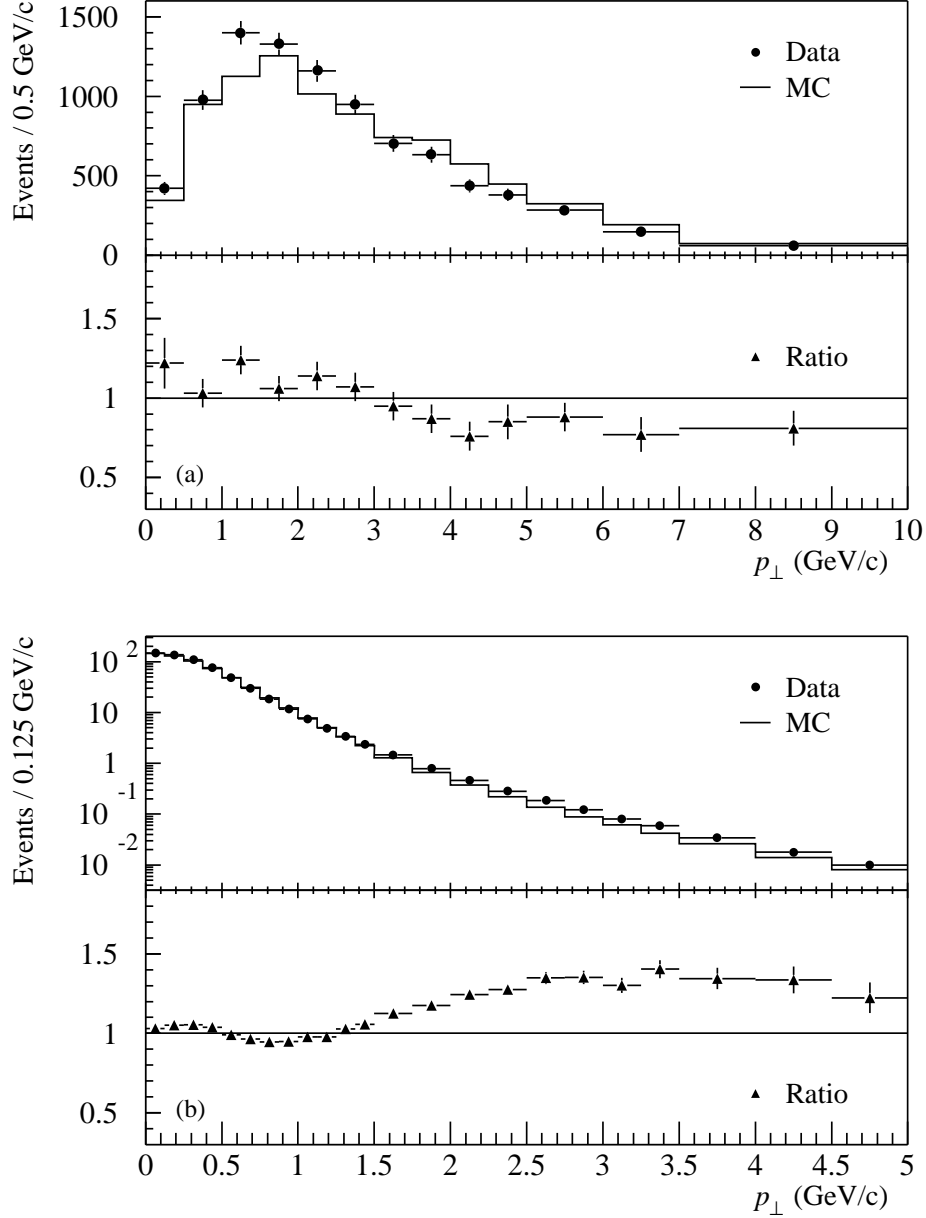
Figure 1: (a) Transverse momentum spectra of fast D* candidates in data and Monte Carlo, along with their ratio. The $p_\perp$ is measured with respect to the remaining tracks of the jet.
(b) Transverse momentum spectra of charged tracks which fulfil the lepton selection kinematic cuts in light–flavour tagged events. The spectra measured in data and Monte Carlo are shown, along with their ratio.
The errors shown account for the limited statistics and the main sources of systematic uncertainties.

cuts, and the spectra of remaining tracks are compared. For charm events, the procedure is the same, the hemisphere tag being provided by a high–energy reconstructed D* ($E_{\mathrm{D}*}/E_{\mathrm{beam}} > 0.5$).

A significant deficit of the order of 20% is found in the Monte Carlo for tracks with $p_\perp > 1.25$ GeV/c in uds events (see Fig. 1b), while the agreement is much better for heavy flavour events. The corrections obtained are used in the analysis, and an uncertainty of 50% is assigned to them, which is much larger than the experimental uncertainty on their determination.

3.7 Identification uncertainties for leptons

The selection efficiencies for the two species of leptons, as well as the background sources, are studied in the data with the technique described in Ref. [3]. In the kinematical region considered, the efficiencies are about 75% and 85% for prompt electrons and muons, respectively. Non–prompt electrons from photon conversions are the main contaminant for the electron sample (2%), while the hadron contamination is significantly lower (0.5%). The muon sample has higher contamination of hadrons (8%) and non–prompt muons from hadron decays (6%). With the statistics available, the precision on the determination of the lepton efficiencies is better than 2%. Relative uncertainties of 20% are assumed on the hadron contamination in both the electron and the muon sample, and on the rate of electrons from photon conversion.

3.8 The background charge correlation

For both the mixing and asymmetry measurements it is useful to distinguish between lepton candidates which cannot possibly carry any information about the original quark charge, (such as electrons from photon conversions or π^0 Dalitz decays, leptons from J/ψ decays, or leptons originating from quarks coming from gluon splitting) and lepton candidates which in principle can retain some "memory" of the original quark charge (high–$p_\perp$ non–prompt or fake leptons, whose decay chain starts with the quark, keep some correlation with the quark charge due to kinematics). It is then useful to define a parameter ξ which gives the probability that a *fake* lepton candidate retains the correct information about the charge of the primary quark in that hemisphere (at the time of decay in the case of b hadrons, *i.e.* after any mixing has occurred). The $\pi/$K relative abundances are modified by the lepton selection (pions are easier to reject, and are less likely to decay in the apparatus), and therefore the charge correlation cannot be correctly evaluated by selecting hadron pairs in the data, since the procedure for selecting a pure sample of hadrons mainly consists of rejecting tracks compatible with the lepton selection. The ξ parameters are measured using the Monte Carlo on a flavour–by–flavour basis, distinguishing between pions and kaons as separate sources of fake or non–prompt leptons, and excluding physical processes which are necessarily charge–symmetric. As expected, it is found that kaons (or leptons coming from kaon decays) in b events are very likely to carry the correct information since they often come from the chain b $\to$ c $\to$ s, where the s quark has the same charge as the b quark, while the opposite holds for charm events. A different behaviour is observed for pions. For $p_\perp > 1.25$ GeV/c the values measured are: $\xi_{\mathrm{K}}^{\mathrm{b}} = 0.84$, $\xi_{\pi}^{\mathrm{b}} = 0.62$, $\xi_{\mathrm{K}}^{\mathrm{c}} = 0.12$, $\xi_{\pi}^{\mathrm{c}} = 0.80$, $\xi_{\mathrm{K}}^{\mathrm{s}} = 0.66$, $\xi_{\pi}^{\mathrm{s}} = 0.55$, $\xi^{\mathrm{d}} = 0.50$, $\xi^{\mathrm{u}} = 0.61$. In the case of Z $\to$ u$\overline{\mathrm{u}}$ and Z $\to$ d$\overline{\mathrm{d}}$ events K and π channels are not separated, since the contribution of these flavours to the high–$p_\perp$ lepton background is negligible.

In order to check the reliability of the Monte Carlo prediction of this effect, opposite–hemisphere hadron pairs are selected using lepton identification criteria as a veto, and the fraction of them which have opposite charge is computed, both in data and Monte Carlo. The comparison shows a

satisfactory agreement. No difference larger than 10% is observed, and a 20% overall uncertainty is assigned to the effect in order to evaluate the systematic error.

4 The mixing measurement

As the lepton charge tags the particle–antiparticle nature of the decaying b hadron, the measurement of the proportion of opposite hemisphere dilepton events which have like sign yields information on the average mixing parameter $\overline{\chi}$, which is defined as the probability that a produced b state decays as a $\overline{\text{b}}$ state. As only neutral B mesons can mix,

$$\overline{\chi} = f_{\text{B}_{\text{d}}^0} \frac{\text{BR}(\text{B}_{\text{d}}^0 \to \ell)}{\text{BR}(\text{b} \to \ell)} \chi_{\text{d}} + f_{\text{B}_{\text{s}}^0} \frac{\text{BR}(\text{B}_{\text{s}}^0 \to \ell)}{\text{BR}(\text{b} \to \ell)} \chi_{\text{s}}$$

where:

- $f_{\text{B}_{\text{i}}^0}$ is the production fraction of B^0 mesons of type i,

- χ_{d} and χ_{s} are the mixing parameters for the $\text{B}_{\text{d}}^0 - \overline{\text{B}}_{\text{d}}^0$ and the $\text{B}_{\text{s}}^0 - \overline{\text{B}}_{\text{s}}^0$ systems.

Starting from the total sample of Z hadronic decays described in Section 2, events are chosen which contain lepton candidates with $p_\perp > 1.25\,\text{GeV}/c$ in both hemispheres of the event, defined in terms of the plane perpendicular to the thrust axis. If a hemisphere contains more than one lepton the one with the highest $p_\perp$ is chosen and the event counted once.

When extracting the mixing parameter, all possible combinations of the following channels in the two hemispheres must be taken into account:

1. $\text{b} \to \ell^-$

2. $\text{b} \to \text{W}^- \to \overline{\text{c}} \to \ell^-$

3. $\text{b} \to \text{c} \to \ell^+$

4. $\text{c} \to \ell^+$

5. fake or non–prompt leptons

where the possibility of having a τ in the decay chain (which does not change the correlation between the lepton candidate and the parent quark charges) has been implicitly included. The first two channels carry the correct information about the b quark sign, while the third one has the wrong correlation. For the non–prompt and fake lepton processes, the probabilities ξ defined in Section 3.8 are used to evaluate each channel's contribution to the like sign sample, assuming that the B_{d}^0 and B_{s}^0 content in these channels is the same as in the prompt–lepton channels. This assumption is supported by the simulation, and the statistical error on the Monte Carlo fractions is used to estimate the corresponding systematic uncertainty.

When extracting the mixing parameter, all possible combinations of the following channels in the two hemispheres must be taken into account:

The various contributions to the like–sign fraction are given in terms of $\overline{\chi}$, in Table 1, for the different lepton sources. The fractions give the dilepton sample composition and depend upon the lepton identification efficiency and the production and decay rates of the channels; they take into account possible correlations between hemispheres, and are obtained from the Monte Carlo simulation after the reweighting procedure described in Section 3.

Flavour	Source			Fraction	Like–sign contribution
b	rs	–	rs	0.819	$2\overline{\chi}(1-\overline{\chi})$
	rs	–	ws	0.103	$\overline{\chi}^2 + (1-\overline{\chi})^2$
	ws	–	ws	0.003	$2\overline{\chi}(1-\overline{\chi})$
	rs	–	bkg	0.032	$\overline{\chi}P_{\mathrm{b}} + (1-\overline{\chi})(1-P_{\mathrm{b}})$
	ws	–	bkg	0.002	$\overline{\chi}(1-P_{\mathrm{b}}) + (1-\overline{\chi})P_{\mathrm{b}}$
	bkg	–	bkg	< 0.001	$2P_{\mathrm{b}}(1-P_{\mathrm{b}})$
c	rs	–	rs	0.002	0
	rs	–	bkg	0.002	$1 - \xi_{\mathrm{c}}$
	bkg	–	bkg	< 0.001	$2\xi_{\mathrm{c}}(1-\xi_{\mathrm{c}})$
uds	bkg	–	bkg	0.002	$2\xi_{\mathrm{uds}}(1-\xi_{\mathrm{uds}})$
any	symmetric			0.035	0.5

Table 1: Contributions to the like–sign fraction from the different channels, along with their relative abundances (which are given for $p_\perp > 1.25$ GeV/c). Under "Source" the origin of the two lepton candidates is given: for prompt leptons those that preserve the charge of the parent quark (after any mixing has occurred in the case of b quarks) are denoted "rs", the others "ws". Background lepton candidates (fake or non–prompt) which can retain some memory of the charge of the quark inside the decaying hadron are denoted "bkg". Pairs in which at least one of the two candidates originate from a charge–symmetric source are grouped together in the last class, irrespective of the parent quark flavour. In the table the probability P_{b} that a lepton candidate of type "bkg" in b events has the same charge as the b quark at production time has been used: $P_{\mathrm{b}} = (1-\overline{\chi})\xi_{\mathrm{b}} + \overline{\chi}(1-\xi_{\mathrm{b}})$.

Given the sample composition and the contribution of each class to the like sign fraction, the average mixing parameter $\overline{\chi}$ is extracted, for a given $p_\perp$ cut, from the proportion of pairs having the same charge. The values obtained are shown in Table 2 with statistical and systematic errors. The cut $p_\perp > 1.25$ GeV/c, giving the minimum total error, is chosen, yielding

$$\overline{\chi} = 0.1246 \pm 0.0051\,_{\mathrm{stat}} \pm 0.0052\,_{\mathrm{syst}}.$$

Details of the contributions to the systematic error are given in the first column of Table 3. The sources and their treatment are discussed in Section 3. Since no angular or momentum distributions are involved in the measurement of the mixing, acceptance effects have little influence on the measured mixing parameter. The largest uncertainties in the measurement come from the lack of knowledge of heavy quark decays.

An important check of the validity of the method comes from study of the dependence of the final results on the $p_\perp$ cut. In Fig. 2a the results quoted in Table 2, obtained with different $p_\perp$ cuts, are plotted along with the uncorrelated errors of each point with respect to the point at the chosen cut of 1.25 GeV/c. No systematic trend is observed.

5   Measurement of $A_{\mathrm{FB}}^{\mathrm{b}}$ and extraction of $\sin^2\theta_{\mathrm{W}}^{\mathrm{eff}}$

For the measurement of $A_{\mathrm{FB}}^{\mathrm{b}}$, hadronic events with at least one identified lepton are accepted. In the case of more than one candidate being found, the one with the largest $p_\perp$ is retained,

$p_\perp$ cut	Lepton pairs		Mixing parameter
(GeV/c)	all	like sign	$\overline{\chi} \pm \Delta\overline{\chi}_{\mathrm{stat}} \pm \Delta\overline{\chi}_{\mathrm{syst}}$
0.75	14478	5135	$0.1264 \pm 0.0054 \pm 0.0113$
1.00	9554	3013	$0.1225 \pm 0.0049 \pm 0.0075$
1.25	6243	1810	$0.1246 \pm 0.0051 \pm 0.0052$
1.50	3876	1053	$0.1243 \pm 0.0059 \pm 0.0040$
1.75	2336	608	$0.1221 \pm 0.0071 \pm 0.0036$

Table 2: Lepton pairs in data and extracted mixing value for various $p_\perp$ cuts. The first quoted error is statistical and the second is systematic.
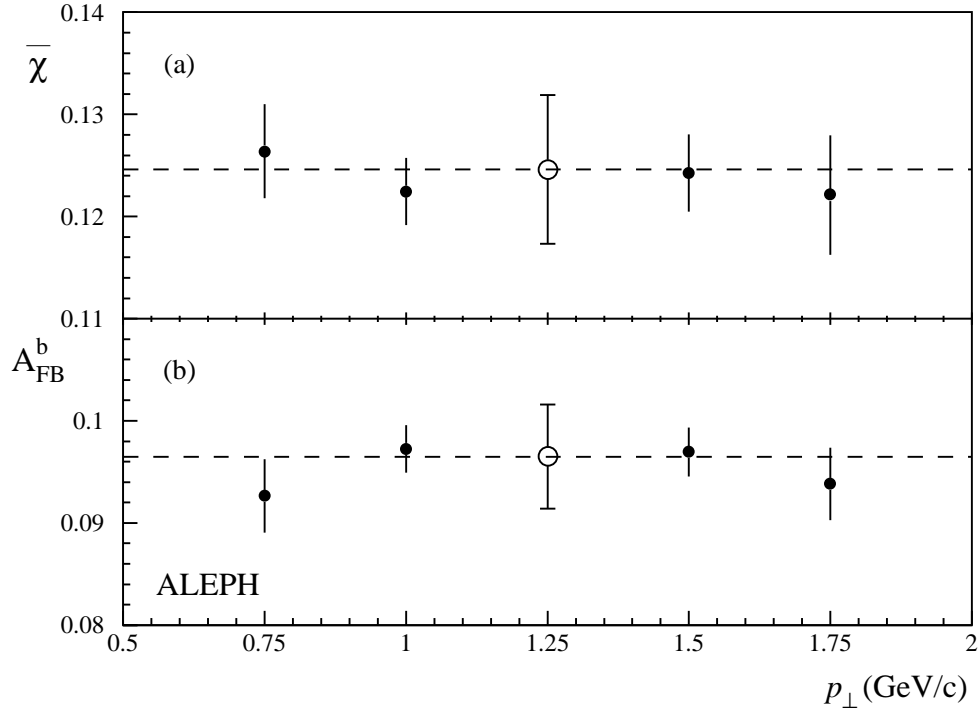

Figure 2: Stability of the mixing (a) and asymmetry (b) measurements with respect to changing the $p_\perp$ cut. The total error is shown at the chosen cut of $p_\perp > 1.25$ GeV/c, while for the other points the uncertainties relate to the difference of each point with respect to the chosen cut. The asymmetry plot refers to data collected at the peak energy.

Source	$\Delta\overline{\chi}$	ΔA_{FB}^{b}
Mixing	–	±0.0015
MC statistics	±0.0020	±0.0002
$BR(b \to \ell)$	±0.0010	∓0.0002
$BR(b \to c \to \ell)$	∓0.0014	∓0.0001
$BR(c \to \ell)$	±0.0002	±0.0005
$BR(b \to W \to c \to \ell)$	±0.0001	< 0.0001
$BR(b \to \tau)$	±0.0003	±0.0001
$BR(b \to u)$	∓0.0008	±0.0001
$BR(b \to J/\psi)$	∓0.0004	< 0.0001
b fragmentation	±0.0007	±0.0005
c fragmentation	∓0.0001	∓0.0012
R_b	±0.0003	∓0.0001
R_c	±0.0001	±0.0010
gluon splitting	∓0.0005	±0.0004
electron ID efficiency	±0.0003	±0.0001
muon ID efficiency	±0.0001	±0.0001
photon conversions	±0.0005	±0.0001
electron background	±0.0003	< 0.0001
punch–through	±0.0011	±0.0004
bkg. $p_\perp$ spectrum	∓0.0001	< 0.0001
charm jets	±0.0001	±0.0008
bkg. charge correlation	∓0.0007	±0.0003
bkg. B^0 content	±0.0004	–
$b \to \ell$ model	$^{-0.0020}_{+0.0019}$	$^{-0.0002}_{+0.0001}$
$c \to \ell$ model	$^{-0.0023}_{+0.0019}$	$^{+0.0007}_{-0.0006}$
$b \to D$ model	$^{-0.0028}_{+0.0023}$	±0.0002
TOTAL	±0.0052	±0.0026

Table 3: Estimated contributions to the systematic uncertainty on $\overline{\chi}$ and A_{FB}^{b}. The various parameters are shifted by $\pm1\sigma$ and the corresponding changes in the measured values are reported. For the modelling sources, the upper and lower variations correspond to the harder and softer spectra, respectively [5].
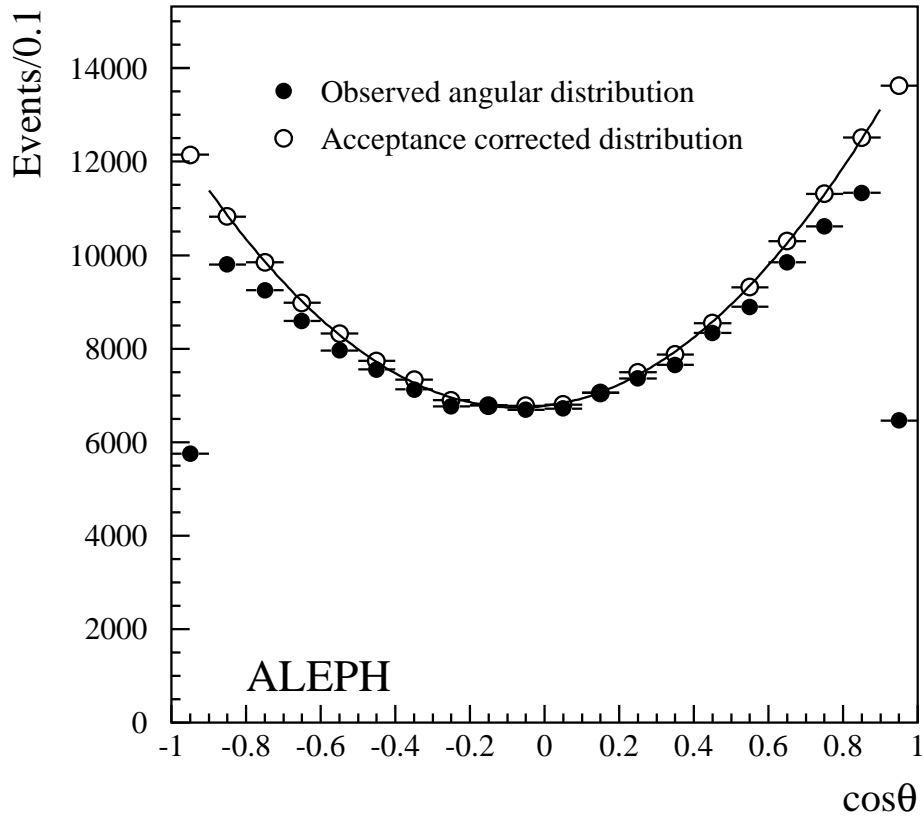
Figure 3: Observed and acceptance–corrected angular distributions at the peak energy. The superimposed curve illustrates the result of the fit.

as it has a higher probability to bring the correct information on the quark charge. Events are classified according to the centre–of–mass energy of the collision, and for each energy the asymmetry measurement is performed.

5.1   Fitting procedure

In the fit for the forward–backward asymmetry, the thrust axis is taken as the experimental estimator of the quark initial direction, as explained in Ref. [3]. The event is divided into hemispheres according to the thrust axis. The axis of the jet containing the lepton is computed, taking into account all charged tracks and neutral objects. The b quark hemisphere is then taken to be that containing the jet axis if the lepton is negatively charged, or the opposite hemisphere otherwise.

The asymmetry value is obtained from an unbinned maximum likelihood fit to the observed $\cos\theta$ distribution of the form

$$\frac{\mathrm{d}\sigma}{\mathrm{d}\cos\theta} = C\left(1 + \cos^2\theta + \frac{8}{3}\mathrm{A}_{\mathrm{FB}}^{\mathrm{obs}}\cos\theta\right).$$

11

$\sqrt{s}$ (GeV)	N_{ev}	$A_{\mathrm{FB}}^{\mathrm{obs}}$	$A_{\mathrm{FB}}^{\mathrm{b}}$
88.38	216	-0.017 ± 0.066	$-0.034 \pm 0.112 \pm 0.007$
89.38	7105	0.034 ± 0.012	$0.053 \pm 0.020 \pm 0.002$
90.21	793	0.051 ± 0.035	$0.089 \pm 0.059 \pm 0.004$
91.21	148,342	0.0533 ± 0.0026	$0.0965 \pm 0.0044 \pm 0.0026$
92.05	1128	0.018 ± 0.030	$0.038 \pm 0.051 \pm 0.002$
92.94	11,174	0.057 ± 0.009	$0.103 \pm 0.016 \pm 0.004$
93.90	502	0.045 ± 0.044	$0.088 \pm 0.075 \pm 0.005$

Table 4: Observed and extracted asymmetry at each centre–of–mass energy. The number of events used in the fit is also shown. For the extracted asymmetry the first error is statistical and the second is systematic.

The observed and acceptance–corrected angular distributions at the peak energy are shown in Fig. 3. The acceptance has been rescaled to one in the bin of maximum efficiency. The first and the last bin show the effect of low acceptance at small polar angles, due mainly to the presence of the beam pipe, and also to the poorer performance of the tracking detectors. Events falling in those two regions ($| \cos \theta | > 0.9$) are not used in the fit. Systematic problems can only arise if detector inhomogeneities are both forward–backward and charge asymmetric. Dimuon and Bhabha pairs reveal no such correlated asymmetry within the apparatus.

In principle the detector acceptance can have some "second order" effects due to the combination of the acceptance itself with the smearing due to physics effects (*e.g.* final state photon and gluon radiation) and detector effects (precision in the thrust axis reconstruction). These effects have been studied using the Monte Carlo, and have been found to be negligible as far as the fit result is concerned.

5.2 Extraction of $A_{\mathrm{FB}}^{\mathrm{b}}$

The asymmetry $A_{\mathrm{FB}}^{\mathrm{obs}}$ is measured at each of the seven energy points, yielding the numbers quoted in Table 4. The measured asymmetry must be corrected for dilution effects to find the true b asymmetry. Corrections arise from:

- leptons resulting from b hadrons which have mixed and therefore have the wrong sign;

- leptons resulting from the cascade decay $b \rightarrow c \rightarrow \ell^+$ which yield the wrong charge and hence the reverse direction for the b quark;

- background from charm and light quark production in the selected sample.

The observed asymmetry can be written as:

$$A_{\mathrm{FB}}^{\mathrm{obs}} = (1 - 2\overline{\chi})(f_{\mathrm{b}}^{\mathrm{rs}} - f_{\mathrm{b}}^{\mathrm{ws}})A_{\mathrm{FB}}^{\mathrm{b}} - f_{\mathrm{c}}A_{\mathrm{FB}}^{\mathrm{c}} + f_{\mathrm{bkg}}A_{\mathrm{FB}}^{\mathrm{bkg}} \qquad (1)$$

where $f_{\mathrm{b}}^{\mathrm{rs}}$ and $f_{\mathrm{b}}^{\mathrm{ws}}$ are the fraction of candidates which are true leptons coming from a b quark, carrying the right and wrong information on the decaying quark charge, respectively; f_{c} is the

$p_\perp$ cut	f_b^{rs}	f_b^{ws}	f_c	$b\overline{b}$ bkg	$c\overline{c}$ bkg	uds bkg	sym bkg
0.75	63.2	8.7	10.2	2.7	1.4	8.7	5.0
1.00	72.9	6.5	6.9	2.1	1.0	6.6	4.0
1.25	79.5	4.6	4.8	1.7	0.7	5.4	3.4
1.50	83.6	3.3	3.5	1.4	0.6	4.6	3.1
1.75	86.1	2.3	2.7	1.2	0.5	4.1	3.0

Table 5: Sample composition (in percent) as a function of the $p_\perp$ cut (in GeV/c). The background component in which some memory of the original quark charge could be retained is split into three different classes, while the charge–symmetric background is not separated.

fraction of prompt leptons from c quarks, f_{bkg} contains all non–prompt or fake candidates, that are not necessarily charge–symmetric (discussed in Section 3.8), and A_{FB}^{bkg} is the corresponding residual asymmetry. The composition fractions are determined from the Monte Carlo simulation, after the reweighting procedure described in Section 3 is applied. The sample composition for different $p_\perp$ cuts is shown in Table 5, where f_{bkg} is split into three classes according to the flavour of the parent quark. The value of $\overline{\chi}$ is taken from the measurement described in Section 4. The value of A_{FB}^c is taken from the Standard Model prediction, but the explicit dependence of the result on A_{FB}^c is given in the final result.

The flavour–dependent charge correlation probabilities ξ discussed in Section 3.8 are used to express the observed background asymmetry as a function of the true quark asymmetries, each of them contributing to the signal via a dilution factor $(2\xi - 1)$:

$$f_{bkg} A_{FB}^{bkg} = \sum_{q=u,d,s,c} \left(\sum_{i=\pi,K} \eta_i^q (2\xi_i^q - 1) \right) A_{FB}^q + \left(\sum_{i=\pi,K} \eta_i^b (2\xi_i^b - 1) \right) (1 - 2\overline{\chi}) A_{FB}^b ,$$

where the η_i^q's are the contributions of the different channels to the total background fraction f_{bkg}.

Equation 1 therefore gives the observed asymmetry A_{FB}^{obs} in terms of the five quark asymmetries, and can be solved for A_{FB}^b, the values of the four lighter quark asymmetries being taken from the Standard Model. The values used are listed in Table 6 as a function of the centre–of–mass energy.

This method has been preferred to simply taking the background asymmetry from the Monte Carlo, mostly because it avoids the inconsistency of using the Monte Carlo b asymmetry to extract the same quantity in the data; moreover, the ξ_i's are determined from a large sample and do not suffer from lack of statistics. For the measured value of A_{FB}^b the method yields $A_{FB}^{bkg} = 0.011 \pm 0.002$ at the peak energy.

5.3 Results

The stability of the extracted value of A_{FB}^b at the peak energy as a function of the $p_\perp$ cut is shown in Fig. 2b. The uncertainties relate to the difference of each point with respect to the chosen cut of 1.25 GeV/c (except for this last point, for which the total error is shown). No trend which could indicate a systematic effect is discernible. The minimum total error is obtained using $p_\perp > 1.25$ GeV/c.

13

$\sqrt{s}$ (GeV)	A_{FB}^u	A_{FB}^d
88.38	−0.0946	0.0343
89.38	−0.0336	0.0588
90.21	0.0055	0.0746
91.21	0.0617	0.0961
92.05	0.0972	0.1101
92.94	0.1251	0.1226
93.90	0.1478	0.1300

Table 6: Standard Model values of the u–type and d–type quark asymmetries used in the extraction of A_{FB}^b, as a function of the centre–of–mass energy.

The contributions to the systematic error are detailed in the second column of Table 3 for the peak value. The systematic error ascribed to the mixing is obtained from the propagation of those uncertainties in the measurement of Section 4 which do not originate from common systematic sources between mixing and asymmetry (the statistical error and the systematic error from Monte Carlo statistics). For the common sources, the effect of the correlation between the two measurements is taken into account.

With the fitting procedure previously described, and the chosen $p_\perp$ cut, the measurement is performed at the seven energy points, yielding the results shown in Table 4 and plotted in Fig. 4. The result of the b asymmetry at peak energy and its dependence on the c asymmetry is given as

$$A_{FB}^b = (0.0965 \pm 0.0044\,_{stat} \pm 0.0026\,_{syst}) \left[1 + 0.0495 \left(\frac{A_{FB}^c - 0.0617}{0.0617} \right) \right].$$

5.4 The extraction of $\sin^2\theta_W^{eff}$

The forward–backward quark asymmetries are related within the Standard Model to the value of the effective electroweak mixing angle. The procedure to unfold QED and QCD [21] effects from the measured b asymmetry, and to correct for the centre–of–mass energy dependence, is fully described in Ref. [5]. The residual dependence on the charm asymmetry is easily handled since the latter can be also expressed in terms of $\sin^2\theta_W^{eff}$ within the Standard Model. The measurement performed can therefore be translated, using all energy points, to a measurement of $\sin^2\theta_W^{eff}$, or, equivalently, of the pole b asymmetry $A_{FB}^0(b)$, yielding

$$
\begin{aligned}
A_{FB}^0(b) &= 0.1008 \pm 0.0043\,_{stat} \pm 0.0028\,_{syst}, \\
\sin^2\theta_W^{eff} &= 0.23198 \pm 0.00092.
\end{aligned}
$$

6 Conclusions

In a sample of about 4,200,000 hadronic Z decays recorded with the ALEPH detector at LEP from 1990 to 1995, the high transverse momentum electrons and muons from semileptonic b decays have been analyzed to measure the b forward–backward asymmetry and the $B^0 - \overline{B}^0$ average
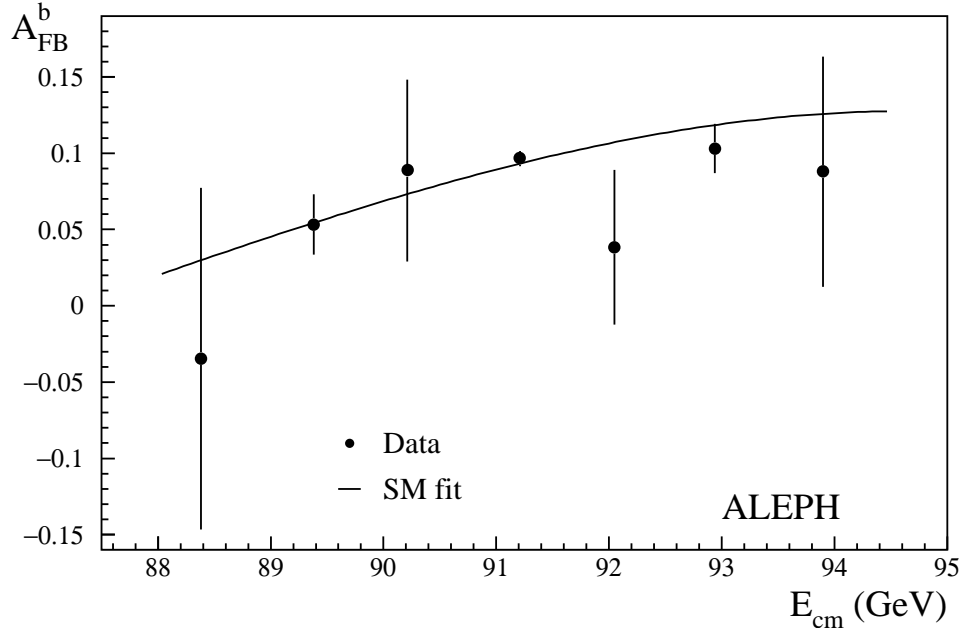
Figure 4: Extracted values of A_{FB}^b as a function of the centre–of–mass energy. The curve shows the Standard Model prediction fitted to the data used for the extraction of $\sin^2\theta_W^{eff}$.

mixing parameter. The values obtained are in agreement with previous ALEPH measurements [22] and with other LEP results [23]. Combining the information coming from the b asymmetry measurements at the seven energy points, and unfolding QED and QCD effects, the value of the pole asymmetry is obtained:

$$A_{FB}^0(b) = 0.1008 \pm 0.0043\,_{stat} \pm 0.0028\,_{syst},$$

corresponding to

$$\sin^2\theta_W^{eff} = 0.23198 \pm 0.00092.$$

The average integrated mixing rate for b hadrons is measured to be

$$\overline{\chi} = 0.1246 \pm 0.0051\,_{stat} \pm 0.0052\,_{syst}.$$

Acknowledgements

We wish to thank our colleagues in the CERN accelerator divisions for the excellent performance of the LEP machine. Thanks are also due to the engineers and technicians at all the collaborating institutions for their contribution to the success of ALEPH. Those of us from non–member states are grateful to CERN for its hospitality.

15

References

[1] ALEPH Coll., D. Decamp *et al.*, Nucl. Instr. Methods **A294** (1990) 121.

[2] ALEPH Coll., D. Buskulic *et al.*, Nucl. Instr. Methods **A360** (1995) 481.

[3] ALEPH Coll., D. Buskulic *et al.*, Nucl. Instr. Methods **A346** (1994) 461.

[4] ALEPH Coll., D. Buskulic *et al.*, Z. Phys. **C62** (1994) 179.

[5] The LEP Experiments: ALEPH, DELPHI, L3 and OPAL, *Combining Heavy Flavour Electroweak Measurements at LEP*, CERN–PPE/96–017, submitted to Nucl. Instr. Methods.

[6] C. Peterson *et al.*, Phys. Rev. **D27** (1983) 105.

[7] ALEPH Coll., D. Buskulic *et al.*, Z. Phys. **C62** (1994) 1.

[8] ALEPH Coll., D. Buskulic *et al.*, Z. Phys. **C62** (1994) 179;
DELPHI Coll., P. Abreu *et al.*, Z. Phys. **C57** (1993) 181;
DELPHI Coll., P. Abreu *et al.*, Z. Phys. **C59** (1993) 533;
L3 Coll., B. Adeva *et al.*, Phys. Lett. **B261** (1991) 177;
OPAL Coll., R. Akers *et al.*, Z. Phys. **C60** (1993) 199;
OPAL Coll., R. Akers *et al.*, Z. Phys. **C60** (1993) 601.

[9] ALEPH Coll., D. Buskulic *et al.*, Phys. Lett. **B357** (1995) 699.

[10] M. Schmitt, *Beauty Semileptonic Branching Ratios*, Proceedings of the 6th International Symposium on Heavy Flavour Physics, Pisa, Italy, June 1995, submitted to Nuovo Cimento.

[11] ALEPH Coll., *Measurement of the semileptonic b branching ratios from inclusive leptons in Z decays*, **EPS0404**, Contribution to the International Europhysics Conference on High Energy Physics, EPS–HEP Brussels, Belgium, July 1995.

[12] CLEO Collab., S. Henderson *et al.*, Phys. Rev. **D45** (1992) 2212.

[13] DELCO Coll., W. Bacino *et al.*, Phys. Rev. Lett. **43** (1979) 1073.

[14] MARK III Coll., R.M. Baltrusaitis *et al.*, Phys. Rev. Lett. **544** (1985) 1976.

[15] CLEO Collab., D. Bortoletto *et al.*, Phys. Rev. **D45** (1992) 21.

[16] CLEO Coll., R. Fulton *et al.*, Phys. Rev. Lett. **64** (1990) 16;
ARGUS Coll., H. Albrecht *et al.*, Phys. Lett. **B234** (1990) 409.

[17] ALEPH Coll., D. Buskulic *et al.*, Phys. Lett. **B343** (1995) 444.

[18] ALEPH Coll., D. Buskulic *et al.*, Phys. Lett. **B295** (1992) 396.

[19] OPAL Collab., R. Akers *et al.*, Phys. Lett. **B353** (1995) 595.

[20] ALEPH Collab., D. Buskulic *et al.*, Phys. Lett. **B313** (1993) 535.

[21] G. Altarelli and B. Lampe, Nucl. Phys. **B391** (1993) 3;
A. Djouadi, B. Lampe and P.M. Zerwas, Z. Phys. **C67** (1995) 123.

[22] ALEPH Coll., D. Buskulic *et al.*, Z. Phys. **C62** (1994) 179;
ALEPH Coll., D. Buskulic *et al.*, Phys. Lett. **B335** (1994) 99.

[23] DELPHI Coll., P. Abreu *et al.*, Z. Phys. **C65** (1995) 569;
DELPHI Coll., P. Abreu *et al.*, Z. Phys. **C66** (1995) 341;
L3 Coll., M. Acciarri *et al.*, Phys. Lett. **B335** (1994) 542;
OPAL Coll., R. Akers *et al.*, Z. Phys. **C60** (1993) 601;
OPAL Coll., R. Akers *et al.*, Z. Phys. **C67** (1995) 365;
OPAL Coll., G. Alexander *et al.*, *Measurement of Heavy Quark Forward–Backward Asymmetries and Average B Mixing Using Leptons in Multihadronic Events*, CERN PPE/95–179, submitted to Z. Phys.